Jurnal Teknologi

Full paper

Ride Comfort Performance Improvement of Electric Vehicle (EV) Conversion Using SAS-Controlled Active Suspension System

Saiful Anuar Abu Bakar[a,*], Ryosuke Masuda[b], Hiromu Hashimoto[c], Takeshi Inaba[b], Hishamuddin Jamluddin[d], Roslan Abdul Rahman[d], Pakharuddin Mohd Samin[a]

[a]*Department of Aeronautical, Automotive and Ocean Engineering, Faculty of Mechanical Engineering, Universiti Teknologi Malaysia, 81310 UTM Johor Bahru, Johor Malaysia*
[b]*Department of Applied Computer Engineering, 4-1-1, Kitakaname, Hiratsuka City, Kanagawa Prefecture 259-1292, Japan*
[c]*Department of Mechanical Engineering, Tokai University, 4-1-1, Kitakaname, Hiratsuka City, Kanagawa Prefecture 259-1292, Japan*
[d]*Department of System Dynamics and Control, Faculty of Mechanical Engineering, Universiti Teknologi Malaysia, 81310 UTM Johor Bahru, Johor Malaysia*

*Corresponding author: saiful@fkm.utm.my

Article history

Received :1 January 2014
Received in revised form : 17August 2014
Accepted :18 August 2014

Graphical abstract

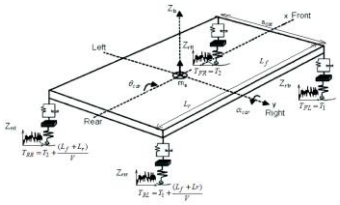

Abstract

This paper presents vehicle's ride comfort performance evaluation after the conversion into an electric vehicle (EV) and the possible ride comfort improvement by an active suspension system have been investigated. The evaluations were done using a validated 7 degrees of freedom of vehicle's ride model. The mathematical modelling of the vehicle's ride as well as its validations was developed in order to predict the vehicle's ride behaviours. The model was then integrated with the active suspension system in order to improve the EV conversion's ride comfort performance. It was found that the modifications towards an EV conversion do not affect vehicle's ride comfort performance significantly, except it changes only the vehicle's vertical displacement, pitch rate and pitch angle responses. However, further application of an active suspension system in EV conversion was found to be able to improve all of the observed responses for ride comfort performance of an EV conversion by overall improvement of 71.1 percent.

Keywords: Electric vehicle; ride comfort performance; active suspension system

1.0 INTRODUCTION

The development of electric vehicle (EV) from the commercially available vehicle model is becoming a trend nowadays due to the global concerns in reducing the greenhouse effect which one of its contributing factors came from the pollution from vehicles. An electric vehicle that is being converted from a normal production vehicle model usually known as an electric vehicle conversion or EV conversion.

The electric vehicle is driven by an electric motor. It is either used only two or four electric motors to move the vehicle. Another common component that can be seen in an electric conversion vehicle are batteries, AC/DC or DC/DC converters, battery management system, pedal relays and others auxiliary components such as electric power steering. Many research works were found to focus on the electric vehicle's electric and electronic systems, but not many were found to focus on improving EV conversion's stability while manoeuvring. The researches on EV conversion's stability are mainly related to the yaw stability control and traction system.

In yaw stability control of electric vehicle [1~4] it focuses on controlling yaw motion of the electric vehicle by controlling the operation of the drive motor. The drive motor, either two or four are basically controlled in termsof its torque generation. While in traction control system [5~8] the generation of electric motor torque is controlled to ensure the wheel does not skid while accelerating ensuring full control over the vehicle. This is done by controlling the slip ratio of the wheel.

It is not clear how the modifications towards an EV conversion affect the vehicle's ride comfort and handling performance; the level of isolations of the passenger compartment from being affected by the harsh road profile and vehicle's steerability after the conversions. Typically, any conversion of an internal combustion engine vehicle to electric vehicle involves

some weight addition (or weight reduction). This is due to the installations of the electric vehicle systems, i.e. battery system and converters. Any weight addition or weight reduction on the chassis will cause the vehicle's weight distribution to change and this can compromise vehicle's ride comfort and handling performance, as the current suspension system tuning was not being designed specifically for the new weight and load distribution at the front and rear axles. This paper will investigate the effects of weight distribution changes on EV conversion's ride comfort when is subjected to random road profiles as well as possible improvements that can be done using an active suspension system.

■2.0 EV CONVERSION RIDE MODEL

The development of seven-degrees-of-freedom (7DOF) vehicle ride model in this study is based on [9] and [10]. The modelling of the simulation model was made based on several assumptions. In developing the mathematical model for an EV conversion it is assumed that vehicle body is lumped into a single mass. This is referred to as the sprung mass. The aerodynamic drag and lift forces are completely ignored in this model. It is also assumed that the vehicle will always remain grounded at all times and the four tyres always in contact with the ground during manoeuvring. The effects of anti-roll bars and the control arm are ignored in this study, to reduce the complexity of the modelling and to prevent simulation error. In modelling the vehicle model, the deflections in pitch and roll planes are small and simplified with small angle approximation. While for the tyre, it is modelled as a linear spring without having damping characteristic.

Figure 1 shows the vehicle model while Figures 2 and 3 shows the model viewed from the front and side of the vehicle respectively.

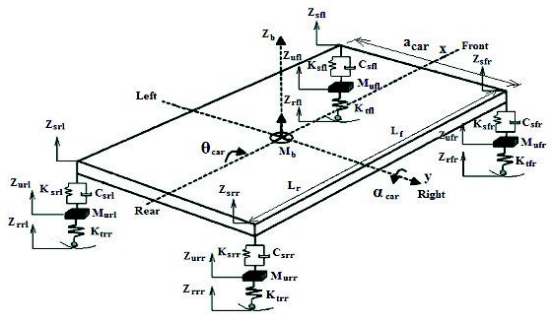

Figure 1 Seven degree of freedom of vehicle ride model

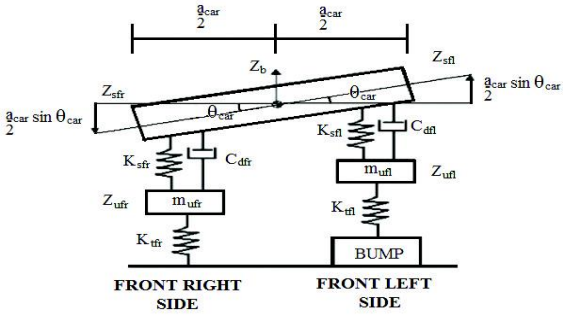

Figure 2 Rolling effect

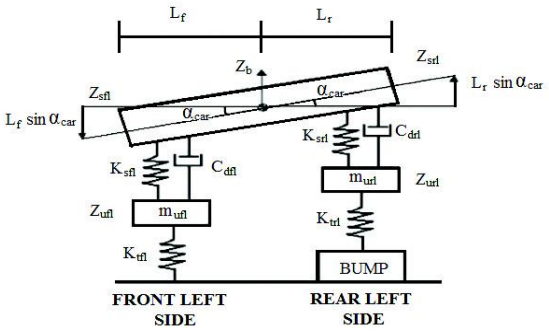

Figure 3 Pitching effect

Based on the 7DOF of ride model in Figures 1 to 3, the displacements of the sprung masses are given by;

$$Z_{sfl} = Z_b + \frac{a_{car}}{2}\theta_{car} - L_f \alpha_{car} \quad (1)$$

$$Z_{sfr} = Z_b - \frac{a_{car}}{2}\theta_{car} - L_f \alpha_{car} \quad (2)$$

$$Z_{srl} = Z_b + \frac{a_{car}}{2}\theta_{car} + L_r \alpha_{car} \quad (3)$$

$$Z_{srr} = Z_b - \frac{a_{car}}{2}\theta_{car} + L_r \alpha_{car} \quad (4)$$

with Z_{sij} is the total sprung mass displacement (i =f for front, r for rear and j=l for left, r for right), Z_b is the sprung mass vertical displacement at the center of gravity, θ_{car} is the roll angle and α_{car} is the pitch angle. The distance of the centre of gravity to the front axle and rear axle are given by L_f and L_r respectively. The value of L_f and L_r are depends on the weight distributions at front and rear axles, where this has not being emphasised in [8] and [9]; the position of the CGthe vehicle's wheelbaselocated at the middle of vehicle's wheelbase. The forces acting on each of the suspension (F_{ij}) is the sum of the spring force (F_{sij}) and damper force (F_{dij}). These suspension forces are given by;

$$F_{fl} = F_{sfl} + F_{dfl} \quad (5)$$

$$F_{fr} = F_{sfr} + F_{dfr} \quad (6)$$

$$F_{rl} = F_{srl} + F_{drl} \quad (7)$$

$$F_{rr} = F_{srr} + F_{drr} \quad (8)$$

In detail, the spring forces in each of the suspension system are given by;

$$F_{sfl} = K_{sfl}(Z_{ufl} - Z_{sfl}) \quad (9)$$

$$F_{sfr} = K_{sfr}(Z_{ufr} - Z_{sfr}) \quad (10)$$

$$F_{srl} = K_{srl}(Z_{url} - Z_{srl}) \quad (11)$$

$$F_{srr} = K_{srr}(Z_{urr} - Z_{srr}) \quad (12)$$

with K_{sij} is the spring stiffness of the spring, Z_{uij} and Z_{sij} are the unsprung mass vertical displacement and the sprung mass vertical displacement respectively at each side of the vehicle. The damper forces are given by

$$F_{dfl} = C_{sfl}(\dot{Z}_{ufl} - \dot{Z}_{sfl}) \quad (13)$$

$$F_{dfr} = C_{sfr}(\dot{Z}_{ufr} - \dot{Z}_{sfr}) \quad (14)$$

$$F_{drl} = C_{srl}(\dot{Z}_{url} - \dot{Z}_{srl}) \quad (15)$$

$$Fdrr = Csr(\dot{Z}urr - \dot{Z}srr) \quad (16)$$

with C_{sij} are the damping coefficient of the dampers, $\dot{Z}_{uij}$ and $\dot{Z}_{sij}$ are the unsprung mass vertical velocity and the sprung mass vertical velocity respectively. For the vehicle tires, it is modelled as a spring and the force acting at the tires is usually known as dynamic tire loads, F_{tij} . For each tire, their dynamic tire loads are given by;

$$F_{tfl} = K_{tfl}(Z_{rfl} - Z_{ufl}) \quad (17)$$

$$F_{tfr} = K_{tfr}(Z_{rfr} - Z_{ufr}) \quad (18)$$

$$F_{trl} = K_{trl}(Z_{rrl} - Z_{url}) \quad (19)$$

$$F_{trr} = K_{trr}(Z_{rrr} - Z_{urr}) \quad (20)$$

where K_{tij} , Z_{rij} , and $Z_{uij,}$ are the tire stiffness, road input displacement and unsprung mass displacement respectively.

Using Newton's Second Law at the vehicle's sprung mass, the body vertical acceleration, $\ddot{Z}_b$ can be determined by

$$F_{fl} + F_{fr} + F_{rl} + F_{rr} = M_b\ddot{Z}_b \quad (21)$$

where M_b is the total mass of the vehicle. Angular acceleration during the roll effect, $\ddot{\theta}$ is given by;

$$(F_{fl} + F_{rl})\frac{a_{car}}{2} - (F_{fr} + F_{rr})\frac{a_{car}}{2} = I_{xx}\ddot{\theta}_{car} \quad (22)$$

where a_{car} is the vehicle's track width and I_{xx} is the moment of inertia about *x*-axis. The angular acceleration while the vehicle is in pitch effect, $\ddot{\alpha}$, it is given by;

$$(F_{rl} + F_{rr})L_r - (F_{fl} + F_{fr})L_f = I_{yy}\ddot{\alpha}_{car} \quad (23)$$

with I_{yy} is moment about *y*-axis . The acceleration of each wheel can be calculated using

$$F_{tfl} - F_{sfl} - F_{dfl} = M_{ufl}\ddot{Z}_{ufl} \quad (24)$$

$$F_{tfr} - F_{sfr} - F_{dfr} = M_{ufr}\ddot{Z}_{ufr} \quad (25)$$

$$F_{trl} - F_{srl} - F_{drl} = M_{url}\ddot{Z}_{url} \quad (26)$$

$$F_{trr} - F_{srr} - F_{drr} = M_{urr}\ddot{Z}_{urr} \quad (27)$$

The ride model of the passenger vehicle was developed using equations (1) to (27) by using Matlab/Simulink.

2.1 Ride Comfort Performance Evaluations on EV Conversion

The developed ride comfort model was used to study the effect of modifications on the passenger vehicle into an electric vehicle. It is assumed in this study that the passenger vehicle is about to be converted into an electric vehicle. The effects of weight distribution in electric vehicle conversion which is typically biased to the rear of the vehicle, due to the battery system are investigated. The evaluations were done by considering two weight distribution ratios; 60:40 and 40:60 weight distribution (WD) ratios. The 60:40 weight distribution ratio is the assumption of weight distribution before modifications while 40:60 weight distribution ratio is the assumption ratio, after modifications are done. The weight distribution used, determined the position of the centre of gravity from the front and rear axles, L_f and L_r respectively. Below are the relation between weight distribution and the distance of CG to front and rear axles:

$$W_f = \frac{W_t}{L}L_r \quad (28)$$

$$W_r = \frac{W_t}{L}L_f \quad (29)$$

where W_f , W_r and W_t are weight at the front axle, weight at the rear axle and vehicle total weight respectively.

■3.0 EV CONVERSION WITH ACTIVE SUSPENSION SYSTEM

An active suspension system is considered in this study to improve EV conversion's ride comfort and handling performance. A slow-active suspension system type is used where it consists a conventional spring combined with hydraulic actuator.

3.1 Modelling of Hydraulic Actuator in Active Suspension System

The modelling of hydraulic actuator for active suspension system is based on [9]. The dynamics of hydraulic actuator is given by

$$\dot{F}_A = A_p\,\alpha\left[C_{d1}\,w u_1\sqrt{\frac{P_s - \mathrm{sgn}(u_1)P_L}{\rho}} - C_{tm}P_L - A_p(\dot{x}_s - \dot{x}_u)\right] \quad (30)$$

where α, C_{d1}, C_{d2} and C_{tm} are constants while A_p , w, $\dot{x}_s - \dot{x}_u$, P_s and P_L are spool length, spool relative velocity, supply pressure and pressure different respectively. Spool valve positions u_1 and u_2 are controlled by a current-position feedback loop.

$$t\dot{u} + u = kv \quad (31)$$

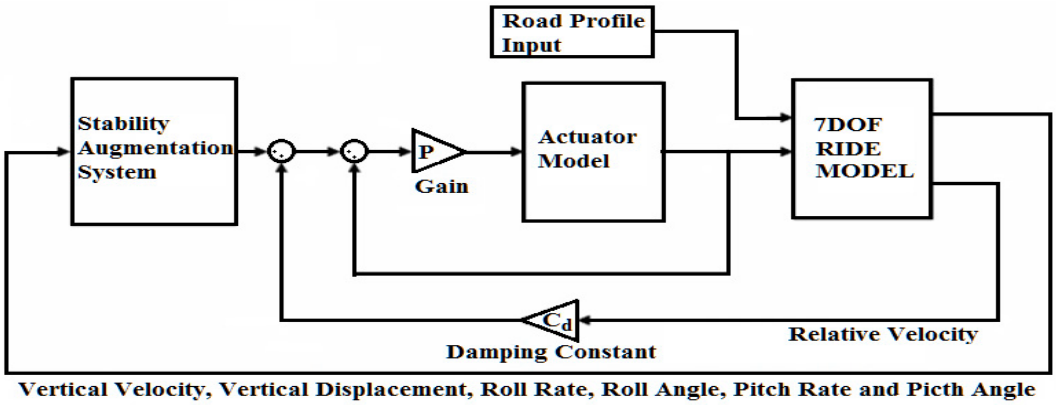

Figure 4 Controller layout for SAS-controlled active suspension system

The parameters of used for hydraulic actuator model were taken from [9] as the followings: Ap= 0.0044 m², α = 2.273e9 N/m5, $Cd1$=0.7, $Cd2$= 0.7, w = 0.008 m, Ps = 20684 kN/m2, ρ =3500, Ctm = 15e-12, τ = 0.001 sec.

3.2 Stability Augmentation System Algorithm

The stability augmentation system (SAS) [10] was used to control the operation of the actuator in active suspension system. The SAS operates by considering the motion of sprung and unsprung mass as well as the vertical roll and pitch motions. The algorithm basically consists of two controller loops; the outer and inner lips. The outer loop is used to reject the effect of road disturbances while the inner loop's function is to stabilize the motions of heave, roll and pitch. Figure 4 shows the controller layout of SAS algorithm in the active suspension system for an EV conversion's ride model. An additional loop is considered in this study, which is the loop of force tracking control. The 2nd inner loop is used for the force tracking control between the estimated damping force from the algorithm and the actual damping force produced by the hydraulic actuator.

The equation of the SAS algorithm is given as follows:

$$\begin{bmatrix} F_{afl} \\ F_{afr} \\ F_{arl} \\ F_{arr} \end{bmatrix} = \begin{bmatrix} \frac{L_r}{2(L_f+L_r)} & -\frac{1}{2(L+L_r)} & \frac{1}{2T} \\ \frac{L_r}{2(L_f+L_r)} & -\frac{1}{2(L+L_r)} & -\frac{1}{2T} \\ \frac{L_f}{2(L_f+L_r)} & \frac{1}{2(L+L_r)} & \frac{1}{2T} \\ \frac{L_f}{2(L_f+L_r)} & \frac{1}{2(L+L_r)} & -\frac{1}{2T} \end{bmatrix} \begin{bmatrix} K_z(Z_{ref}-Z_s)-B_z\dot{Z}_s \\ K_q(q_{ref}-q)-B_q\dot{q} \\ K_a(a_{ref}-a)-B_a\dot{a} \end{bmatrix} + C_d \begin{bmatrix} (\dot{Z}_{ufl}-\dot{Z}_{sfl}) \\ (\dot{Z}_{ufr}-\dot{Z}_{sfr}) \\ (\dot{Z}_{url}-\dot{Z}_{srl}) \\ (\dot{Z}_{urr}-\dot{Z}_{srr}) \end{bmatrix} \quad (32)$$

where $K_z, K_\theta, K_\alpha, B_z, B_\theta, B_\alpha$, and C_d are constants (for the outer loop) and damping coefficient (for the inner loop) respectively.

The parameter value in the SAS algorithm can either be tuned manually or by using any available optimization method, towards an optimal ride comfort performance i.e. genetic algorithm optimization method. In this study, a systematic tuning procedure is used, in tuning the parameter values in the SAS algorithm. The tuning was done by focusing the search for parameter value in the outer loop, followed by the 1st inner loop and 2nd inner loop. Figure 5 shows flow for the parameter values tuning in SAS algorithm.

1. 1st Inner Loop Tuning
   Once the values of K and B was confirmed to give the lowest value of CRMS for heave, roll and pitch, the tuning in searching the value of the damping coefficient, C_d is started. Table 2 is used to assist the tuning effort for the 1st inner loop.

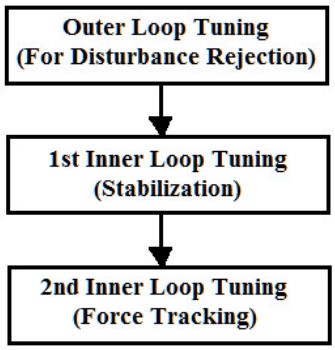

Figure 5 Manual tuning procedures for SAS algorithm

2. 2nd Inner Loop Tuning
   The 2nd inner loop is used for the purpose of force tracking control. Based on the rigorous work it was found that only proportional gain, P affects the force tracking in the simulation model. Table 3 is used to assist the tuning effort for the 2nd inner loop.

Based on the tuning work done, it was found that the value for K and B is 1e6 and 1e5 respectively. The tuning done for 1st inner loop gave the value for C_d is 0. As the value of P (in the 2nd loop) is 18.

Table 1 Tuning table for the SAS system's outer loop

Kz\Bz	0	10	100	1000	10000	100000
0	CRMS1	CRMS8	CRMS15	CRMS22	CRMS29	CRMS36
10	CRMS2	CRMS9	CRMS16	CRMS23	CRMS30	CRMS37
100	CRMS3	CRMS10	CRMS17	CRMS24	CRMS31	CRMS38
1000	CRMS4	CRMS11	CRMS18	CRMS25	CRMS32	CRMS39
10000	CRMS5	CRMS12	CRMS19	CRMS26	CRMS33	CRMS40
100000	CRMS6	CRMS13	CRMS20	CRMS27	CRMS34	CRMS41
1000000	CRMS7	CRMS14	CRMS21	CRMS28	CRMS35	CRMS42

Table 2 Tuning table for the SAS system's 1st inner loop

Cd (Ns/m)	0	100	200	300	400	500	600	700	800	900	1000
CRMS	CRMS1	CRMS2	CRMS3	CRMS4	CRMS5	CRMS6	CRMS7	CRMS8	CRMS9	CRMS10	CRMS11

Table 3 Tuning table for the SAS system's 2nd inner loop

P	0	1	2	3	...	...	...	...	18	19	20
CRMS	CRMS1	CRMS2	CRMS3	CRMS4	...	...	...	...	CRMS18	CRMS19	CRMS20

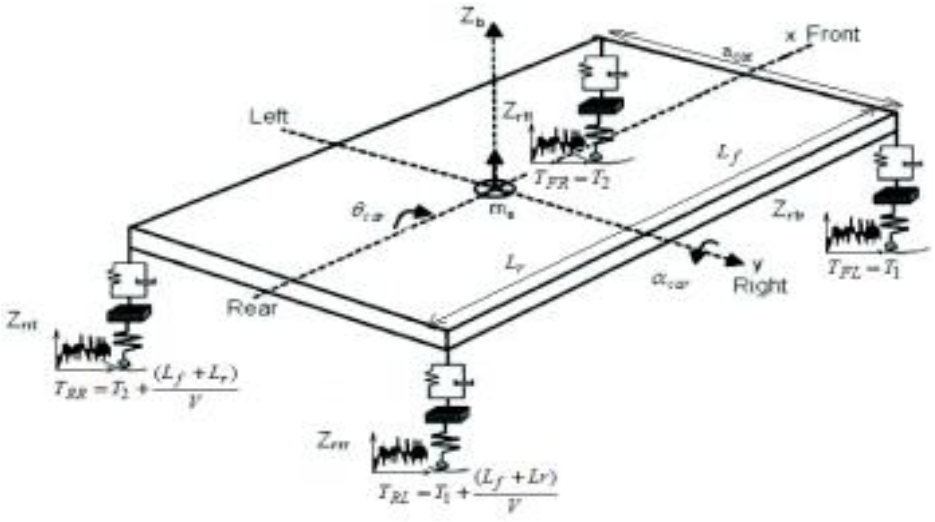

Figure 6 Random road profile input

4.0 RANDOM ROAD PROFILES INPUT

The random road profiles were used to simulate the EV conversion ride comfort performance when it is driven on a rough terrain. The worst case scenario of road profiles for the EV conversion was selected due to the fact that the developed simulation model has been validated to be reliable in representing roll and pitch behaviour of the vehicle. Figure 6 shows the diagram of timing of random road profiles, subjected to the simulation model.

The random road profiles of the simulation model were generated based on the timing of front and rear wheels hit the road profiles. It is assumed that at the front wheel the inputs were generated at the time equal to T while the rear wheels will only have the same input as the front wheel after a while, which is at the time is equal to $T+(L_f+L_r)/V$. However, in order to create the roll and pitch effect simultaneously, the timing for left and right side of the vehicle need to be slightly different. Below are the timing for the inputs given to the simulation model

$$T_{FL}=T_1 \quad (33)$$

$$T_{FR}=T_2 \quad (34)$$

$$T_{RL}=T_1+\frac{(L_f+Lr)}{V} \quad (35)$$

$$T_{RR}=T_2+\frac{(L_f+L_r)}{V} \quad (36)$$

with T_{FL}, T_{FR}, T_{RL} and T_{RR} are the hitting time for the front left, front right, rear left and rear right wheels respectively.

5.0 SIMULATION RESULTS

Table 4 shows the ride comfort performance of the vehicle before the conversion, after the conversion as well as the EV conversion's responses with the active suspension system. Based on Table 4, it can be seen that that there are no significant changes occurred on the observed responses as the result of the modifications towards an EV; except for the vertical displacement response for both of the vehicle models. It seems that the modification into an electric vehicle is causing the vehicle to have a higher vertical displacement peak when the vehicle is subjected to the random road profiles input. Pitch motions (pitch rate and pitch angle) were also observed to change. This is happening due to position changing of the CG. In a normal vehicle, the CG is located near the front axle and when the wheel hit the bump, the vertical displacement peak would be higher, compared when the rear wheel hit the bump. As for the EV conversion, the CG is biased to the rear axle, therefore when the front wheel hit the bump; the vertical displacement magnitude peak is not as high when the rear wheel hit the bump.

As for the improvement made by the active suspension system, it is observed that in general the active suspension system was able to improve all the observed responses for EV conversion ride behaviours. The most significant improvement that made by the active suspension system are in improving the vertical displacement and roll angle responses of the vehicle. The active suspension system controlled by the SAS algorithm functions by lifting up the vehicle when the wheels in the pothole

Table 4 RMS values of the studied responses during random road profiles input

	60:40WD	40:60WD	Active (40:60)	Improvement Over 40:60WD (%)
Jerk (m/s³)	248.4	249.2	0.9226	99.6
Vertical Acceleration (m/s²)	1.544	1.5444	0.384	75.1
Vertical Displacement (m)	0.007492	0.007714	0.000275	96.4
Roll Rate (rad/s)	0.002313	0.0002398	0.002187	8.8
Roll Angle (rad)	0.0006160	0.0006170	0.0001131	81.7
Pitch Rate (rad/s)	0.0034730	0.0037490	0.002107	43.8
Pitch Angle (rad)	0.0005553	0.0005598	0.00004424	42.1

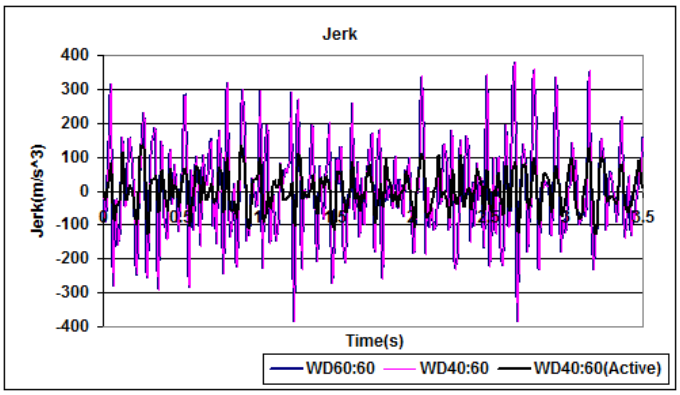

Figure 7 Jerk responses

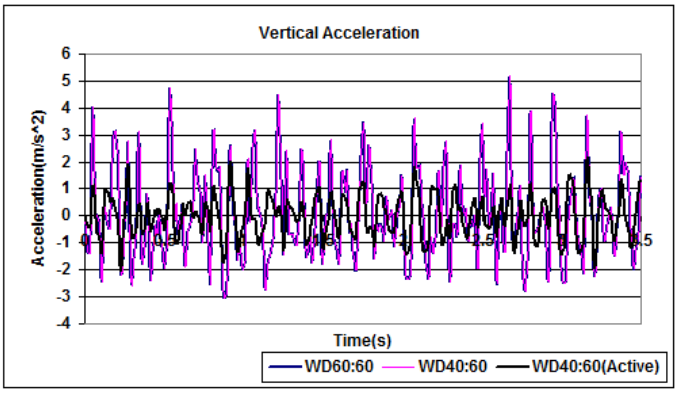

Figure 8 Vertical acceleration responses

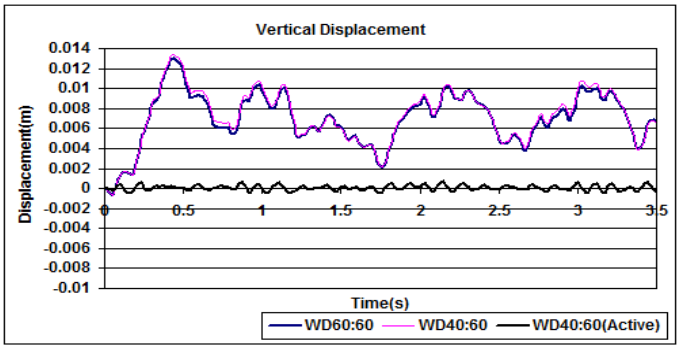

Figure 9 Vertical displacement responses

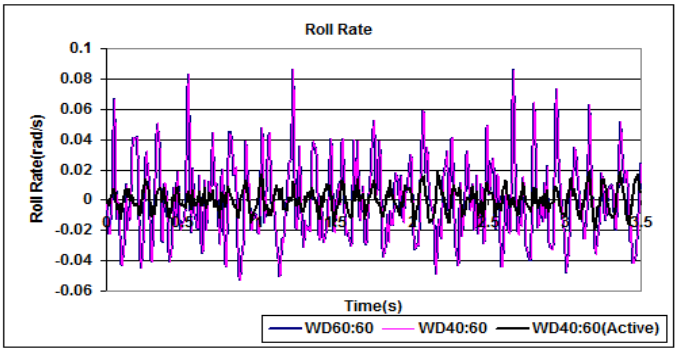

Figure 10 Roll rate responses

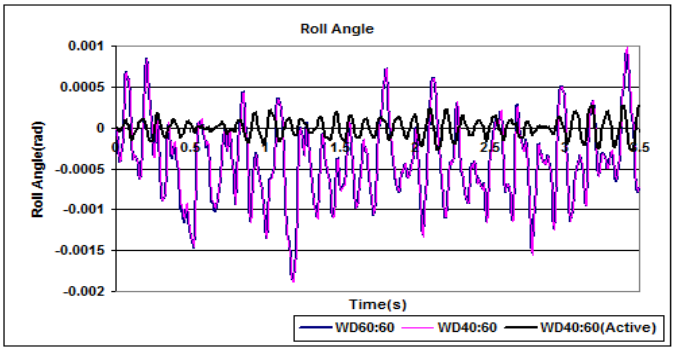

Figure 11 Roll angle responses

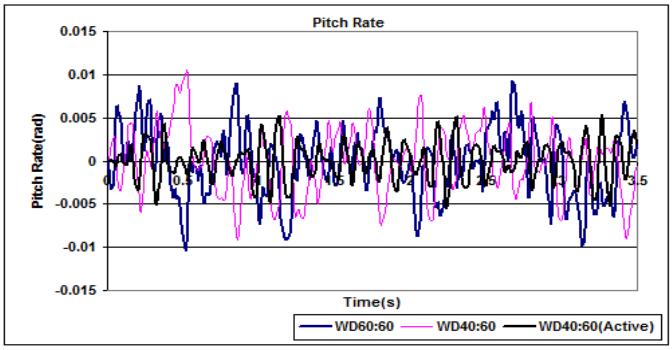

Figure 12 Pitch rate responses

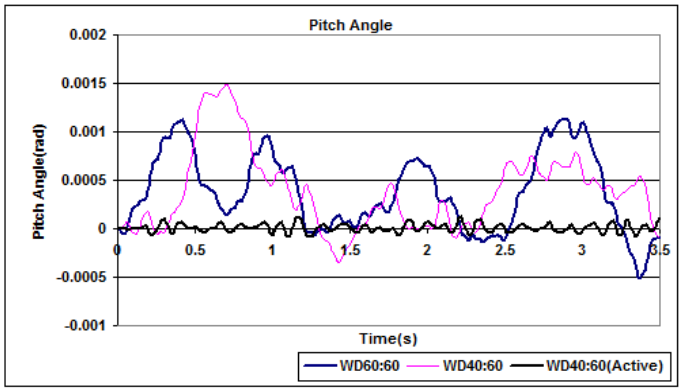

Figure 13 Pitch angle responses

6.0 CONCLUSIONS

The modification of a normal passenger vehicle into an electric vehicle was found not to significantly affect the vehicle's ride comfort performance. The application of active suspension system in an electric vehicle conversion was found to significantly improve the vehicle's ride comfort performance. However, electric vehicle conversion's ride comfort improvement made by the active suspension would be depending on the algorithm used to control the operations of the actuators in the active system. The SAS used to control the hydraulic actuator in active suspension system was found to be able to improve the ride comfort performance of the EV conversion significantly

Acknowledgement

The authors wish to acknowledge the financial support of Ministry of Science, Technology and Innovation, Malaysia, PROTON Malaysia for the donation of PROTON PERSONA which was used as the experimental car and finally the staffs of the Department of Aeronautical, Automotive and Ocean Engineering, Faculty of Mechanical Engineering, Universiti Teknologi Malaysia.

References

[1] C. Zou, H. Zhou, and Z. He. 2014. The Research of Wheel Drive Vehicle Yaw Stability Controller Based on Model Predictive Control. *Advanced Materials Research*. 998–999: 735–740.

[2] L. Zheng, & J. Ye. 2014. Analysis of the Lateral Stability for Four-Wheel Independent Driving Electric Vehicles. In *Applied Mechanics and Materials*.590:394–398

[3] F. Tahami, R. Kazemi, and S. Farhanghi. 2003. A Novel Driver Assist Stability System for All-Wheel-Drive Electric Vehicles. *IEEE Transactions on Vehicular Technolog*. 52: 683–692.

[4] S. Zheng, H. Tang, Z. Han, and Y. Zhang. 2006. Controller Design for Vehicle Stability Enhancement. *Control Engineering Practice*. 14: 1413–1421.

[5] K. Jeongmin, and K. Hyunsoo. 2007. Electric Vehicle Yaw Rate Control Using Independent in-Wheel Motor. *Power Conversion Conference.* April 2–5. Nagoya, Japan.

[6] H. Sado, S. Sakai, and Y. Hori. 1999. Road Condition Estimation for Traction Control in Electric Vehicle. *Proceedings of the IEEE International Symposium on Industrial Electronics.* Bled, Slovenia, Jul 12-16.

[7] J. Yamakawa, and K. Watanabe. 2006. A Method of Optimal Wheel Torque Determination for Independent Wheel Drive Vehicles. *Journal of Terramechanics*. 43:269–285.

[8] J. Yamakawa, A. Kojima, and K. Watanabe. 2007. A Method of Torque Control for Independent Wheel Drive Vehicles on Rough Terrain. *Journal of Terramechanics*. 44:370–381.

[9] K. Hudha, H. Jamaluddin, P.M. Samin, and R.A. Rahman. 2003. Vehicle Modelling and Validations: Experience with Proton Car. *International Association of Vehicle System Dynamics (IAVSD)*. August 24–30. Kanagawa, Japan.

[10] P.M. Samin, H. Jamaluddin, R.A. Rahman, S. Anuar, and K. Hudha, 2008. Semi-Active Suspension System For Handling Quality and Longitudinal Stability Improvements Using Hybrid Stability Augmentation System-Force Control Algorithm. *2nd Regional Conference on Vehicle Engineering and Technology*. 15–16 July. Kuala Lumpur, Malaysia.

[11] M.D. Donahue. 2001. *Implementation of an Active Suspension and Preview Controller for Improved Ride Comfort.* University of California at Berkeley: MSc. Dissertation.